

# Complete conformal classification of the Friedmann-Lemaître-Robertson-Walker solutions with a linear equation of state II

Tomohiro Harada,<sup>1,\*</sup> Takahisa Igata,<sup>2,†</sup> Takuma Sato,<sup>1,‡</sup> and Bernard Carr<sup>3,§</sup>

<sup>1</sup>*Department of Physics, Rikkyo University, Toshima, Tokyo 171-8501, Japan*

<sup>2</sup>*KEK Theory Center, Institute of Particle and Nuclear Studies,*

*High Energy Accelerator Research Organization, Tsukuba 305-0801, Japan*

<sup>3</sup>*School of Physics and Astronomy,*

*Queen Mary University of London,*

*Mile End Road, London E1 4NS, United Kingdom*

(Dated: October 27, 2021)

## Abstract

We completely classify the Friedmann-Lemaître-Robertson-Walker solutions with spatial curvature  $K = 0, \pm 1$  for perfect fluids with linear equation of state  $p = w\rho$ , where  $\rho$  and  $p$  are the energy density and pressure for the perfect fluid without assuming any energy conditions. We study the qualitative behaviour of all geodesics and the structure of conformal boundaries with an emphasis on parallelly propagated curvature singularities and draw the Penrose diagrams for all cases. As for the future singularity, if  $\rho > 0$ , the spacetime commonly ends up with a big-rip spacelike singularity for  $w < -1$ , although it is still future null geodesically complete for  $-5/3 \leq w < -1$ . For the past singularity with  $K = 0, -1$ , if  $\rho > 0$ , the spacetime begins with a big-bang spacelike singularity for  $w > -1/3$ , a big-bang null singularity for  $-1 < w \leq -1/3$  and a non-scalar polynomial curvature null singularity for  $-5/3 < w < -1$ . Therefore, an inflationary universe with  $K = 0, -1$  for  $-5/3 < w < -1/3$  has an initial singularity unless  $w = -1$ . For  $K = 1$  and  $-1 < w < -1/3$ , however, the solution describes a bouncing universe, where the initial singularity is removed. The spacetime for  $K = -1$  and  $w \leq -5/3$  is past extendible beyond its initial null boundary. It turns out that for  $K = 0, -1$ ,  $w > -5/3$  and  $\rho > 0$ , no spacelike geodesic emanates from or terminates at the spacelike infinity.

---

\* harada@rikkyo.ac.jp

† igata@post.kek.jp

‡ stakuma@rikkyo.ac.jp

§ b.j.carr@qmul.ac.uk

## CONTENTS

I. Introduction	3
II. The FLRW spacetime	4
A. Conformal completion	4
B. FLRW solutions with $p = w\rho$	6
III. Geodesics, spacelike curves and the Riemann tensor	8
A. Geodesics and spacelike curves	8
B. Riemann tensor	11
IV. Structure of conformal boundary	12
A. Definitions	12
B. Flat FLRW solutions	14
C. Positive-Curvature FLRW solutions	17
D. Negative-Curvature FLRW solutions with $\rho \geq 0$	18
E. Negative-Curvature FLRW solutions with $\rho < 0$	21
V. Summary	23
Acknowledgments	24
A. Integrals	25
References	25

## I. INTRODUCTION

The Friedmann-Lemaître-Robertson-Walker (FLRW) spacetime is unique as a spatially homogeneous and isotropic spacetime [1]. The FLRW metric has spatial curvature  $K = 0, \pm 1$  and it is generally accepted that this, together with the Einstein equation, approximately describes our Universe very well. For the matter content, a perfect fluid with linear equation of state  $p = w\rho$  is often adopted, where  $\rho$ ,  $p$  and  $w$  are the energy density, pressure and a constant parameter, respectively. Observationally, recent cosmological observations strongly suggest the acceleration of the cosmological expansion. This needs dark energy, which can be parameterised by a linear equation of state with  $w < -1/3$ . The observations require  $w = -1.00_{-0.05}^{+0.04}$  [2] and spatial curvature  $\Omega_K = 0.000 \pm 0.005$  [3].

As concrete examples for the linear equations of state,  $w = 1/3, 0$  and  $-1$  correspond to radiation fluid, dust and a cosmological term, respectively. Phenomenologically,  $w = 1, -1/3$  and  $-2/3$  correspond to a massless scalar field (or stiff fluid), a string network and a domain wall network, respectively. The ranges  $-1/3 < w < -1$  and  $w < -1$  correspond to quintessence [4, 5] and a phantom field [6], respectively. It should be also noted that viable modified theories of gravity may contain effective Einstein equation which violates the null energy condition [7]. The FLRW spacetime not only provides a realistic model of our Universe but also plays an important role as a piece of an exact solution. The most famous example is the Oppenheimer-Snyder solution [8], which describes gravitational collapse to a black hole, where the FLRW solution describes a metric inside the collapsing uniform ball. The FLRW spacetime is also used as a piece of a model for the formation of a primordial black hole [9, 10] and a stable gravastar [11, 12].

The conformal structures and singularities are the basic properties of any spacetime. The Penrose diagrams for the FLRW solutions for  $-1 < w < 1$  are summarised in [13]. The possibility of big-rip singularities has been proposed in [14–16]. The behaviour of geodesics around singularities in the FLRW spacetime has been analysed in detail in [17]. Recently, the past extendibility of inflationary FLRW universe has been discussed in [18, 19]. In [20], which we will refer to as Paper I, all of the FLRW solutions with  $p = w\rho$  are given without assuming any energy conditions and then the corresponding Penrose diagrams are drawn by studying only null and comoving timelike geodesics, scalar polynomial (s.p.) curvature singularities, trapped regions and trapping horizons. In this paper, we extend this analysis

to include all geodesics and parallelly propagated (p.p.) curvature singularities. We use the units in which  $c = G = 1$  and the abstract index notation in Wald's textbook [1] throughout this paper.

## II. THE FLRW SPACETIME

### A. Conformal completion

The line element in the FLRW spacetime is written in the following form:

$$\begin{aligned} ds^2 &= -dt^2 + a^2(t)[dr^2 + \Sigma_K^2(r)d\Omega^2] \\ &= a^2(\eta)[-d\eta^2 + dr^2 + \Sigma_K^2(r)d\Omega^2], \end{aligned} \quad (2.1)$$

where  $a > 0$ ,  $ad\eta = dt$ ,  $d\Omega^2 = d\theta^2 + \sin^2\theta d\phi^2$  with  $0 \leq \theta \leq \pi$  and  $0 \leq \phi < 2\pi$ , and

$$\Sigma_K(r) = \begin{cases} r & (K = 0) \\ \sin r & (K = 1) \\ \sinh r & (K = -1) \end{cases} . \quad (2.2)$$

Depending on the spatial curvature, the domain of the coordinates  $(r, \eta)$  is given by

$$-\infty < \eta < \infty, \quad 0 \leq r < \infty \quad (\text{for } K = 0, -1), \quad 0 \leq r \leq \pi \quad (\text{for } K = 1), \quad (2.3)$$

unless  $\eta$  is further restricted to a smaller interval by the specific solution.

The conformal completion is a prescription to deal with the ‘‘boundary’’ of the spacetime. If the spacetime  $M$  is conformally isometric to a bounded open region of the ‘‘unphysical’’ spacetime  $\tilde{M}$ , the boundary of the image of  $M$  in  $\tilde{M}$  is called the conformal boundary [1, 21]. The line element in the flat FLRW spacetime can be rewritten as

$$ds^2 = \frac{1}{4}a^2(\eta) \sec^2\left(\frac{\tau + \chi}{2}\right) \sec^2\left(\frac{\tau - \chi}{2}\right) (-d\tau^2 + d\chi^2 + \sin^2\chi d\Omega^2), \quad (2.4)$$

where

$$\tau = \arctan(\eta + r) + \arctan(\eta - r), \quad \chi = \arctan(\eta + r) - \arctan(\eta - r). \quad (2.5)$$

Thus, the physical spacetime is conformally isometric to the bounded region  $\chi \geq 0$ ,  $\tau - \chi > -\pi$  and  $\tau + \chi < \pi$  in the Einstein static universe. The domain of  $(\chi, \tau)$  is plotted in

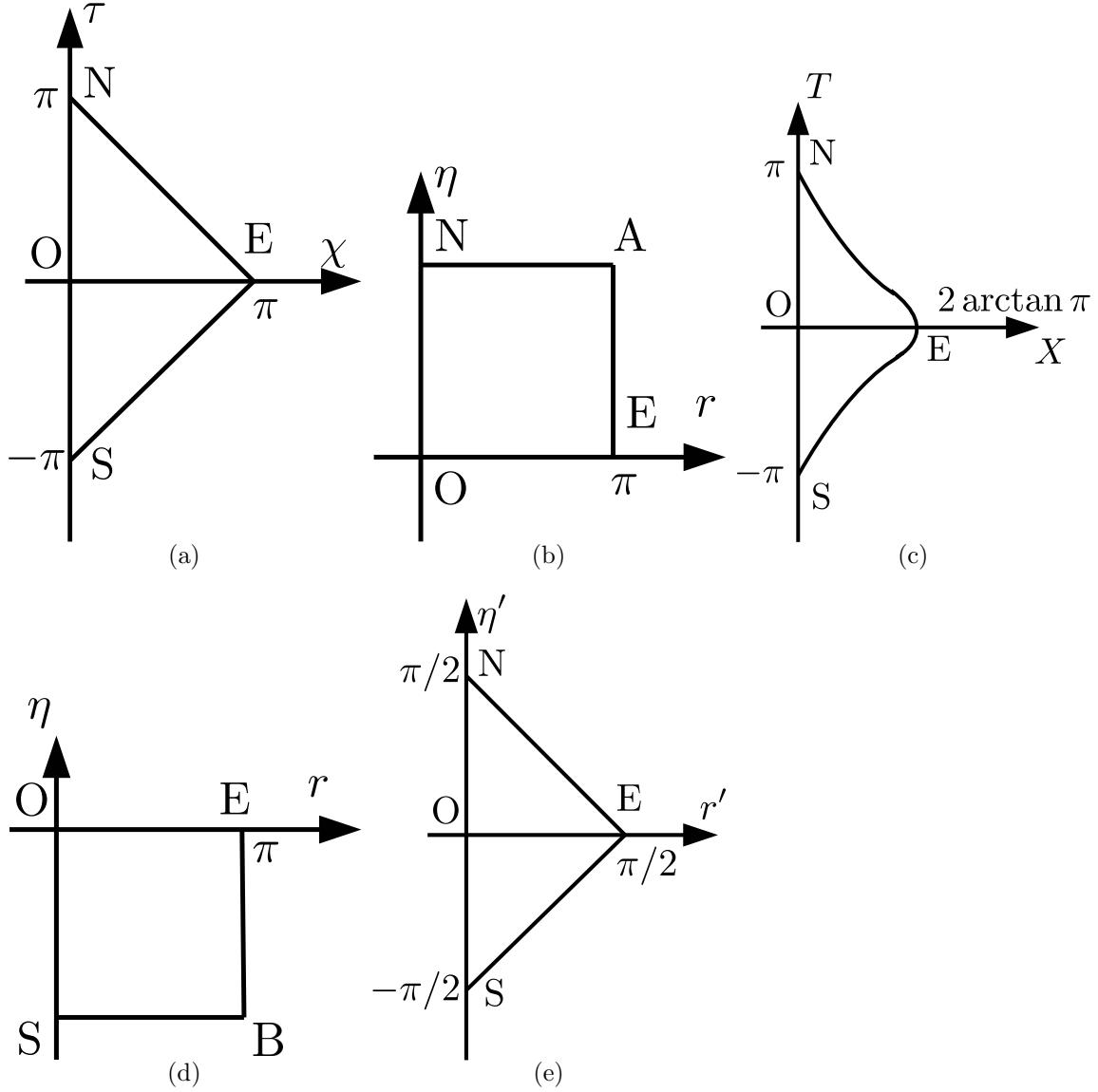


FIG. 1. The domain of the coordinate planes for (a) the flat case, the positive-curvature cases for (b)  $w > -1/3$ , (c)  $w = -1/3$  and (d)  $w < -1/3$ , and (e) the negative-curvature case.

Fig. 1(a), where the coordinates  $(\chi, \tau)$  of O, N, E and S are  $(0, 0)$ ,  $(0, \pi)$ ,  $(\pi, 0)$  and  $(0, -\pi)$ , respectively.

For the positive-curvature case, as we will see later, the domain of  $\eta$  depends on the parameter  $w$ . For  $w > -1/3$  and  $w < -1/3$ , the domains are restricted to the bounded intervals  $0 < \eta < 2\pi/(1 + 3w)$  and  $2\pi/(1 + 3w) < \eta < 0$ , respectively. Since the domain of  $r$  is also bounded, the domains of  $(r, \eta)$  for  $w > -1/3$  and  $w < -1/3$  are as plotted in Figs. 1(b) and 1(d), respectively. In Fig. 1(b), the coordinates  $(r, \eta)$  of O, N, A and E are

$(0, 0)$ ,  $(0, 2\pi/(1 + 3w))$ ,  $(\pi, 2\pi/(1 + 3w))$  and  $(\pi, 0)$ , respectively, while in Fig. 1(d), those of O, E, B and S are  $(0, 0)$ ,  $(\pi, 0)$ ,  $(\pi, 2\pi/(1 + 3w))$  and  $(0, 2\pi/(1 + 3w))$ , respectively. For  $w = -1/3$ , however, the domain of  $\eta$  is not bounded. In this exceptional case, in which  $-\infty < \eta < \infty$ , we can use the line element

$$ds^2 = \frac{1}{4}a^2(\eta) \sec^2 \frac{T+X}{2} \sec^2 \frac{T-X}{2} \times \left( -dT^2 + dX^2 + 4 \cos^2 \frac{T+X}{2} \cos^2 \frac{T-X}{2} \sin^2 r d\Omega^2 \right), \quad (2.6)$$

where

$$T = \arctan(\eta + r) + \arctan(\eta - r), \quad X = \arctan(\eta + r) - \arctan(\eta - r). \quad (2.7)$$

Thus, the physical spacetime is conformally isometric to the bounded region

$$X \geq 0, \quad -\pi < T < \pi, \quad \tan \frac{T+X}{2} - \tan \frac{T-X}{2} \leq 2\pi, \quad (2.8)$$

as plotted in Fig. 1(c), where the coordinates  $(X, T)$  of O, N, E and S are  $(0, 0)$ ,  $(0, \pi)$ ,  $(2 \arctan \pi, 0)$  and  $(0, -\pi)$ , respectively.

For the negative-curvature case, the line element can be rewritten as

$$ds^2 = \frac{a^2(\eta)}{\cos(r' + \eta') \cos(r' - \eta')} (-d\eta'^2 + dr'^2 + \sin^2 r' d\Omega^2), \quad (2.9)$$

where

$$\tan \eta' = \frac{\sinh \eta}{\cosh r}, \quad \tan r' = \frac{\sinh r}{\cosh \eta}. \quad (2.10)$$

The original domain is mapped to the bounded region

$$r' \geq 0, \quad \eta' - r' > -\frac{\pi}{2}, \quad \eta' + r' < \frac{\pi}{2}. \quad (2.11)$$

Thus, the physical spacetime is conformally isometric to a bounded region in the Einstein static universe as plotted in Fig. 1(e), where the coordinates  $(r', \eta')$  of O, N, E and S are  $(0, 0)$ ,  $(0, \pi/2)$ ,  $(\pi/2, 0)$  and  $(0, -\pi/2)$ , respectively.

## B. FLRW solutions with $p = w\rho$

If we now assume the Einstein equation, the matter field turns out to have the perfect-fluid form

$$T^{ab} = (\rho + p)u^a u^b + pg^{ab}, \quad (2.12)$$

where  $\rho$ ,  $p$  and  $u^a := a^{-1}(\partial/\partial\eta)^a$  are the energy density, pressure and four-velocity of the fluid element, respectively. If we further assume  $p = w\rho$  with  $w = \text{const}$ , the conservation law  $\nabla^a T_{ab} = 0$  implies

$$\rho = \rho_0 \left(\frac{a_0}{a}\right)^{3(1+w)}, \quad (2.13)$$

where  $\rho = \rho_0$  when  $a = a_0$ . For  $w \neq -1/3$ , the Einstein equation reduces to

$$\left(\frac{d\tilde{a}}{d\tilde{t}}\right)^2 = \frac{\tilde{a}_c}{\tilde{a}} - K, \quad (2.14)$$

where

$$\tilde{a} := a^{1+3w}, \quad d\tilde{t} := (1+3w)\tilde{a}^{3w/(1+3w)}dt, \quad \tilde{a}_c := \frac{8\pi}{3}\rho_0 a_0^{3(1+w)}. \quad (2.15)$$

For  $w = -1/3$ , it reduces to

$$\left(\frac{da}{dt}\right)^2 = \tilde{a}_c - K, \quad (2.16)$$

where

$$\tilde{a}_c := \frac{8\pi}{3}\rho_0 a_0^2. \quad (2.17)$$

For the vacuum case, only  $K = 0$  and  $K = -1$  are possible. For  $K = 0$ , the solution is  $a = a_0 = \text{const}$ , corresponding to Minkowski spacetime, while for  $K = -1$ , it is  $a = e^\eta$ , corresponding to Milne spacetime. For the non-vacuum case, we first consider  $w \neq -1/3$ . For  $K = 0$  and  $\rho > 0$ , Eq. (2.14) is integrated to give

$$a(\eta) = \begin{cases} b_0\eta^\alpha & \text{for } 0 < \eta < \infty & (w > -1/3) \\ b_0(-\eta)^\alpha & \text{for } -\infty < \eta < 0 & (w < -1/3), \end{cases} \quad (2.18)$$

where  $\alpha = 2/(1+3w)$  and  $b_0$  is a positive constant. This class contains Einstein-de Sitter universe ( $w = 0$ ) and de Sitter spacetime in the flat chart ( $w = -1$ ). For  $K = 1$ , the energy density must be positive and Eq. (2.14) is integrated to give

$$\tilde{a} = \tilde{a}_c \frac{1 - \cos \tilde{\eta}}{2}, \quad \tilde{t} = \tilde{a}_c \frac{\tilde{\eta} - \sin \tilde{\eta}}{2} \quad (2.19)$$

with  $\eta = \tilde{\eta}/(1+3w)$ , which contains de Sitter spacetime in the global chart ( $w = -1$ ). For  $K = -1$  and  $\rho > 0$ , Eq. (2.14) is integrated to give

$$\tilde{a} = \tilde{a}_c \frac{\cosh \tilde{\eta} - 1}{2}, \quad \tilde{t} = \tilde{a}_c \frac{\sinh \tilde{\eta} - \tilde{\eta}}{2}, \quad (2.20)$$

which contains de Sitter spacetime in the open chart ( $w = -1$ ), while for  $K = -1$  and  $\rho < 0$ ,

$$\tilde{a} = \tilde{a}'_c \frac{1 + \cosh \tilde{\eta}}{2}, \quad \tilde{t} = \tilde{a}'_c \frac{\tilde{\eta} + \sinh \tilde{\eta}}{2} \quad (2.21)$$

with  $\tilde{a}'_c = -\tilde{a}_c$ , which contains anti-de Sitter spacetime in the open chart ( $w = -1$ ). For the  $w = -1/3$  non-vacuum case, Eq. (2.16) again implies that the energy density can be negative only for  $K = -1$ . For  $\tilde{a}_c - K > 0$ , Eq. (2.16) is integrated to give  $a = b_c e^{b_c \eta}$ , where  $b_c = \sqrt{\tilde{a}_c - K}$ , while for  $\tilde{a}_c - K = 0$ , the solution is static as  $a = a_0 = \text{const.}$

### III. GEODESICS, SPACELIKE CURVES AND THE RIEMANN TENSOR

#### A. Geodesics and spacelike curves

Due to the symmetry, without loss of generality, we only have to consider geodesics in the two-dimensional timelike plane  $\theta = \pi/2$  and  $\phi = 0$ . The Lagrangian then takes the simplified form

$$L = \frac{1}{2} a^2(\eta)(-\dot{\eta}^2 + \dot{r}^2), \quad (3.1)$$

where the dot denotes differentiation with respect to the affine parameter  $\lambda$ . In addition, the Euler-Lagrange equations are

$$\frac{d}{d\lambda}(a^2 \dot{\eta}) + a a'(-\dot{\eta}^2 + \dot{r}^2) = 0, \quad (3.2)$$

$$\frac{d}{d\lambda}(a^2 \dot{r}) = 0, \quad (3.3)$$

where the prime denotes differentiation with respect to  $\eta$ . The above equations are integrated to give

$$\dot{r} = \frac{C}{a^2}, \quad (3.4)$$

$$a^2(-\dot{\eta}^2 + \dot{r}^2) = D, \quad (3.5)$$

where  $C$  and  $D$  are constants. We can normalise  $D$  so that  $D = 0, 1$  and  $-1$  for the null, spacelike and timelike geodesics, respectively. Clearly,  $r$  has no turning point.

If we take  $\eta = \eta(\lambda)$ , Eqs. (3.4) and (3.5) reduce to the one-dimensional potential form

$$\dot{\eta}^2 + V_\eta(\eta) = 0; \quad V_\eta(\eta) = -\frac{C^2}{a^4(\eta)} + \frac{D}{a^2(\eta)}. \quad (3.6)$$

This implies that  $\eta$  has no turning point for  $D = 0, -1$ , while the allowed region is given by  $a(\eta) \leq |C|$  for  $D = 1$  and there can be a turning point at  $\eta = \eta_{tp}$ , where  $a(\eta_{tp}) = |C|$ . As  $r = 0$  is a regular centre,  $C$  becomes  $-C$  as the geodesic passes through there.

We classify geodesics as follows.

(i) Null geodesic ( $D = 0$ ): We take the affine parameter to have  $\dot{\eta} > 0$ . Equation (3.5) is integrated to give

$$\eta - \eta_0 = \pm(r - r_0), \quad (3.7)$$

where  $\eta = \eta_0$  when  $r = r_0$ . We can make  $C = \pm 1$  by an affine transformation so that

$$\lambda - \lambda_0 = \int_{\eta_0}^{\eta} a^2(\tilde{\eta}) d\tilde{\eta}, \quad (3.8)$$

where  $\lambda = \lambda_0$  when  $\eta = \eta_0$ .

(ii) Timelike geodesic ( $D = -1$ ): We again take  $\dot{\eta} > 0$ , giving two cases.

(ii-a) Comoving timelike geodesic (CTG) ( $C = 0$ ): Equations (3.4) and (3.5) are integrated to give

$$\lambda - \lambda_0 = \int_{\eta_0}^{\eta} a(\tilde{\eta}) d\tilde{\eta} = t - t_0, \quad r = r_0. \quad (3.9)$$

(ii-b) Non-comoving timelike geodesic (NCTG) ( $C \neq 0$ ): Equations (3.4) and (3.5) are integrated to give

$$\lambda - \lambda_0 = \int_{\eta_0}^{\eta} \frac{a(\tilde{\eta}) d\tilde{\eta}}{\sqrt{1 + (C/a(\tilde{\eta}))^2}}, \quad (3.10)$$

$$r - r_0 = \int_{\eta_0}^{\eta} \frac{C d\tilde{\eta}}{\sqrt{a^2(\tilde{\eta}) + C^2}}. \quad (3.11)$$

The latter can be transformed to

$$(\eta - \eta_0) - \sigma(r - r_0) = \int_{\eta_0}^{\eta} \left( 1 - \frac{1}{\sqrt{1 + (a(\tilde{\eta})/C)^2}} \right) d\tilde{\eta}, \quad (3.12)$$

where  $\sigma = \text{sgn}(dr/d\eta)$ .

(iii) Spacelike geodesic ( $D = 1$ ): Equation (3.6) implies  $C \neq 0$ , so  $a(\eta)$  cannot be greater than  $|C|$  along spacelike geodesics. This gives two cases.

(iii-a) Instantaneous spacelike geodesic (ISG): We assume  $\eta = \eta_0 = \text{const}$ . In this case, Eqs. (3.2) and (3.6) immediately imply  $a'(\eta_0) = 0$  and  $C = \pm a(\eta_0)$ . Equation (3.4) is integrated to give  $\lambda - \lambda_0 = C(r - r_0)$ .

(iii-b) Non-instantaneous spacelike geodesic (NISG): The geodesic equations are integrated to give

$$\lambda - \lambda_0 = \sigma_{\eta} \int_{\eta_0}^{\eta} \frac{a(\tilde{\eta}) d\tilde{\eta}}{\sqrt{(C/a(\tilde{\eta}))^2 - 1}}, \quad (3.13)$$

$$r - r_0 = \sigma_{\eta} \int_{\eta_0}^{\eta} \frac{C}{\sqrt{C^2 - a^2(\tilde{\eta})}} d\tilde{\eta}, \quad (3.14)$$

where  $\sigma_\eta = \text{sgn}(\dot{\eta})$ . The latter equation can be transformed to

$$\eta - \eta_0 - \sigma(r - r_0) = - \int_{\eta_0}^{\eta} \left( \frac{1}{\sqrt{1 - (a(\tilde{\eta})/C)^2}} - 1 \right) d\tilde{\eta}, \quad (3.15)$$

where  $\sigma = \text{sgn}(dr/d\eta)$ .

(iv) Instantaneous spacelike curve (ISC): We consider a spacelike curve given by  $\eta = \eta_0$ . This is not a geodesic unless  $a'(\eta_0) = 0$ . The generalised affine parameter (g.a.p.) plays an important role in defining the b-boundary [21, 22]. If we choose the proper length  $s = ar$  as a parameter along the curve, the tangent vector is given by  $k^a = a^{-1}(\partial/\partial r)^a$ , where  $a = a(\eta_0)$ . Then, the p.p. basis  $\{e_{(\alpha)}^a\}_{\alpha=0,1,2,3}$ , which satisfies  $k^a \nabla_a e_{(\alpha)}^b = 0$ , is given by

$$\begin{aligned} e_{(0)}^a &= \cosh\left(\frac{a'}{a}r\right) a(d\eta)^a + \sinh\left(\frac{a'}{a}r\right) a(dr)^a, \\ e_{(1)}^a &= \sinh\left(\frac{a'}{a}r\right) a(d\eta)^a + \cosh\left(\frac{a'}{a}r\right) a(dr)^a, \\ e_{(2)}^a &= a\Sigma_K(r)(d\theta)^a, \quad e_{(3)}^a = a\Sigma_K(r) \sin\theta(d\phi)^a, \end{aligned} \quad (3.16)$$

where  $a = a(\eta_0)$  and  $a' = a'(\eta_0)$ . Since

$$k^{(0)} = -\sinh\left(\frac{a'}{a}r\right), \quad k^{(1)} = \cosh\left(\frac{a'}{a}r\right), \quad k^{(2)} = k^{(3)} = 0, \quad (3.17)$$

where  $k^a = k^{(\alpha)}e_{(\alpha)}^a$ , the g.a.p. of this curve is given by the following integral:

$$u = \int_0^s \left[ \sum_{\alpha=0}^3 (k^{(\alpha)})^2 \right]^{1/2} (\tilde{s}) d\tilde{s} = a \int_0^r \sqrt{\cosh\left(2\frac{a'}{a}\tilde{r}\right)} d\tilde{r}. \quad (3.18)$$

Although this integral does not admit a compact expression in terms of elementary functions, it can be easily shown that the asymptotic form of the g.a.p. is given by

$$u \approx \begin{cases} ar & (2|a'|r/a \ll 1) \\ \frac{a^2}{\sqrt{2}|a'|} e^{|a'|r/a} & (2|a'|r/a \gg 1) \end{cases}. \quad (3.19)$$

Only null and comoving timelike geodesics were studied in Paper I but here we extend the analysis to all geodesics and ISCs.

## B. Riemann tensor

Since the FLRW spacetime is conformally flat, the Weyl tensor identically vanishes and the Riemann tensor is determined by the Ricci tensor, whose components in the coordinates  $(\eta, r, \theta, \phi)$  are

$$R_{00} = Aa^2, \quad Aa^2 = -3\mathcal{H}', \quad (3.20)$$

$$R_{0i} = 0, \quad (3.21)$$

$$R_{ij} = Ba^2\gamma_{ij}, \quad Ba^2 = \mathcal{H}' + 2\mathcal{H}^2 + 2K, \quad (3.22)$$

where  $\mathcal{H} := a'/a$  and  $i$  and  $j$  run over 1, 2 and 3. Therefore, the Ricci tensor can be written in the form

$$R^{ab} = Aa^2(d\eta)^a(d\eta)^b + Ba^2\gamma_{ij}(dx^i)^a(dx^j)^b. \quad (3.23)$$

This can be then rewritten as

$$R^{ab} = Ae_{(0)}^a e_{(0)}^b + B\delta^{ij}e_{(i)}^a e_{(j)}^b, \quad (3.24)$$

where  $\{e_{(\alpha)}^a\}_{\alpha=0,1,2,3}$  is a natural tetrad basis given by

$$e_{(0)}^a = -a(d\eta)^a, \quad e_{(1)}^a = a(dr)^a, \quad e_{(2)}^a = a\Sigma_K(r)(d\theta)^a, \quad e_{(3)}^a = a\Sigma_K(r)\sin\theta(d\phi)^a. \quad (3.25)$$

Since any scalar curvature polynomial is written as a polynomial of  $A$  and  $B$ , such as  $R = -A + 3B$  and  $R^{ab}R_{ab} = A^2 + 3B^2$ , the boundedness of  $A$  and  $B$  implies that of all scalar curvature polynomials.

To examine curvature singularities, we need to construct a p.p. basis along the pertinent curves. For CTGs, the p.p. pseudo-orthonormal basis is given by Eq. (3.25) and the Ricci tensor in the p.p. frame is given by Eq. (3.24). For null geodesics with a tangent vector  $k^a$ , the p.p. frame basis is given by

$$k^a = [-(d\eta)^a \pm (dr)^a]/\sqrt{2}, \quad l^a = a^2[-(d\eta)^a \mp (dr)^a]/\sqrt{2}, \quad (3.26)$$

where  $e_{(2)}^a$  and  $e_{(3)}^a$  are the same as in Eq. (3.25). These basis vectors satisfy

$$k^a k_a = 0, \quad l^a l_a = 0, \quad k^a l_a = -1, \quad k^a e_{(A)a} = 0, \quad l^a e_{(A)a} = 0, \quad g^{ab}e_{(A)a}e_{(B)b} = \delta_{AB}, \quad (3.27)$$

where  $A$  and  $B$  run over 2 and 3. Using this basis, the Ricci tensor can be written as

$$R^{ab} = \frac{A+B}{2}a^2 \left( k^a k^b + \frac{1}{a^4} l^a l^b \right) + \frac{A-B}{2}(k^a l^b + l^a k^b) + B\delta^{AB}e_{(A)a}^a e_{(B)b}^b. \quad (3.28)$$

For general non-null geodesics with a tangent vector  $k^a$ , the p.p. pseudo-orthonormal basis is given by

$$e_{(0)}^a = k^a = a^2[-k^0(d\eta)^a + k^1(dr)^a], \quad e_{(1)}^a = a^2[-k^1(d\eta)^a + k^0(dr)^a], \quad (3.29)$$

where  $e_{(2)}^a$  and  $e_{(3)}^a$  are the same as in Eq. (3.25). In terms of this basis, the Ricci tensor is

$$\begin{aligned} R^{ab} = & \left[ (A+B)\frac{C^2}{a^2} - AD \right] e_{(0)}^a e_{(0)}^b \pm (A+B)\frac{C}{a} \sqrt{\frac{C^2}{a^2} - D} (e_{(0)}^a e_{(1)}^b + e_{(1)}^a e_{(0)}^b) \\ & + \left[ (A+B)\frac{C^2}{a^2} - BD \right] e_{(1)}^a e_{(1)}^b + B\delta^{AB} e_{(A)}^a e_{(B)}^b, \end{aligned} \quad (3.30)$$

so the result for the CTGs is recovered if we take  $C = 0$  and  $D = -1$ .

The Einstein equation directly means

$$A + B = 8\pi(\rho + p), \quad B = 4\pi(\rho - p). \quad (3.31)$$

Thus, from the result in the previous section, an incomplete geodesic corresponds to an s.p. curvature singularity if and only if  $\rho$  or  $p$  is unbounded along the geodesic. Using the conservation law, together with the equation of state  $p = w\rho$ , we find

$$A + B = 8\pi(1+w)\rho_0 \left(\frac{a_0}{a}\right)^{3(1+w)}, \quad B = 4\pi(1-w)\rho_0 \left(\frac{a_0}{a}\right)^{3(1+w)}. \quad (3.32)$$

## IV. STRUCTURE OF CONFORMAL BOUNDARY

### A. Definitions

If a component of the Riemann tensor in the p.p. frame is unbounded along an incomplete geodesic, it corresponds to a curvature singularity. This is also called a p.p. or a  $\mathbf{C}^{0-}$  curvature singularity [21, 22] and implies the inextendibility of the spacetime within the class with  $C^{2-}$  metric tensor. If a scalar curvature polynomial is unbounded along the geodesic, it corresponds to an s.p. curvature singularity. This is a p.p. curvature singularity but not vice versa. If it is not an s.p. curvature singularity, it is called a non-s.p. curvature singularity. Here we consider the image of a curve in  $M$  under the conformal transformation to the unphysical spacetime  $\tilde{M}$ . Given an inextendible spacetime, if an incomplete geodesic terminates at a point on the conformal boundary of  $M$ , we call this ‘‘endpoint’’ a spacetime singularity.

Our discussion of the Riemann tensor in the p.p. frame for geodesics in the FLRW spacetime implies the following. As for an incomplete CTG, a p.p. curvature singularity is an s.p. curvature singularity from Eq. (3.24). This applies for an incomplete null geodesic if and only if

$$(A + B)a^2, (A + B)a^{-2}, A - B, \text{ or } B \quad (4.1)$$

is unbounded, from Eq. (3.28), and for an incomplete non-null general geodesic if and only if

$$(A + B)\frac{C^2}{a^2} - AD, (A + B)\frac{C}{a}\sqrt{\frac{C^2}{a^2} - D}, (A + B)\frac{C^2}{a^2} - BD, \text{ or } B \quad (4.2)$$

is unbounded, from Eq. (3.30). Paper I only covered s.p. curvature singularities, while the current paper includes p.p. curvature singularities.

Before studying the structure of conformal boundary of the FLRW solutions, we need to clarify some definitions. If a complete null (timelike) geodesic in  $M$  terminates at a point in the conformal boundary, we call this point null (timelike) infinity. If there is a point in the conformal boundary that is spacelike-related to all points in  $M$  and is also the endpoint of a b-complete spacelike curve in  $M$ , we call it a spacelike infinity. So null (timelike) infinities are infinities for null (timelike) geodesics, while the spacelike infinities are infinities for spacelike but not causal geodesics or curves. We denote the null, timelike and spacelike infinities as  $\mathcal{I}^\pm$ ,  $i^\pm$  and  $i^0$ , respectively.<sup>1</sup> If there is a point in the conformal boundary that is not a p.p. curvature singularity and is the endpoint of an incomplete geodesic, we call it an extendible boundary. Although the above definitions may not suffice to classify the conformal boundaries of all possible spacetimes, they suffice for the classification of the FLRW spacetimes under consideration. Note that if the spacetime  $M$  is extendible, the above definition of spacelike infinities crucially depends on whether it is further extended or not. In the following, we restrict our attention to the spacetime region described by the FLRW solutions discussed in Sec. II, even if it is extendible.

For FLRW spacetimes, we call an s.p. curvature singularity at  $t = t_s$  a big-bang (big-crunch) singularity if  $a \rightarrow 0$  and  $|\rho| \rightarrow \infty$  as  $t \rightarrow t_s \pm 0$ . We call an s.p. curvature singularity at  $t = t_s$  a future (past) big-rip singularity if  $a \rightarrow \infty$  and  $|\rho| \rightarrow \infty$  as  $t \rightarrow t_s \mp 0$ .<sup>2</sup>

---

<sup>1</sup> These terminology and notation are not the same as in [21], where infinities for null geodesics in de Sitter spacetime are termed as spacelike infinities but denoted by  $\mathcal{I}^\pm$ .

<sup>2</sup> There was a typo in the corresponding definition in Paper I.

## B. Flat FLRW solutions

First we discuss the flat case since this provides the basics for other cases. The domains of  $\eta$  are then  $0 < \eta < \infty$ ,  $-\infty < \eta < \infty$  and  $-\infty < \eta < 0$  for  $w > -1/3$ ,  $w = -1/3$  and  $w < -1/3$ , respectively. Since the result for  $w \geq -1$  is well known, we will focus on  $w < -1$  below. Some useful integrals are shown in Appendix A.

For null geodesics, as seen from Eq. (3.8), the affine parameter  $\lambda$  is determined by the integrals given by Eq. (A2). For  $w < -1$ , in the limit  $\eta \rightarrow 0$ , which corresponds to the segment OE in Fig. 1(a),  $\lambda$  goes to positive infinity for  $-5/3 \leq w < -1$ , while it is finite for  $w < -5/3$ . Therefore, we identify OE with future null infinity for  $-5/3 \leq w < -1$  but a big-rip singularity for  $w < -5/3$ . As the past boundary  $\eta = -\infty$  and  $r = \infty$ , which corresponds to ES, is approached,  $\lambda$  is finite for  $-5/3 < w < -1$  but goes to negative infinity for  $w \leq -5/3$ . For  $-5/3 < w < -1$ , both  $A$  and  $B$  are bounded, while  $(A + B)/a^2$  is unbounded, implying that ES is identified with a non-s.p. curvature singularity. For  $w \leq -5/3$ , ES is identified with past null infinity  $\mathcal{I}^-$ .

Next we consider CTGs. As seen from Eq. (3.9),  $\lambda$  is determined by the integrals given by Eq. (A1). For  $w < -1$ , the future boundary  $\eta = 0$ , which corresponds to OE, is a big-rip singularity. The past boundary  $\eta = -\infty$ , which corresponds to S, is a past timelike infinity  $i^-$ .

Let us proceed to NCTGs. First we focus on the future boundary  $\eta = 0$ . As seen from Eq. (3.10),  $\lambda$  is determined by the integrals given by Eq. (A1) and it is finite for  $w < -1$ . From Eqs. (3.11) and (3.12), both  $r$  and  $\eta - \sigma r$  remain finite in this limit. Therefore, the NCTGs terminate at OE but not E. Both  $A$  and  $B$  are unbounded, implying that OE corresponds to a big-rip singularity. Next, we consider the past boundary  $\eta = -\infty$ . As seen from Eq. (3.10),  $\lambda$  is determined by the integrals given by Eq. (A2). It is finite for  $-5/3 < w < -1$  but goes to negative infinity for  $w \leq -5/3$ . From Eq. (3.12),  $\eta + r$  remains finite for  $-5/3 < w < -1$  but goes to negative infinity for  $w \leq -5/3$ . For  $-5/3 < w < -1$ ,  $A$  and  $B$  are bounded but  $(A + B)/a^2$  is unbounded. Therefore, for  $-5/3 < w < -1$ , the NCTGs emanate from a non-s.p. curvature singularity on ES but neither E nor S, while for  $w \leq -5/3$  from S, past timelike infinity  $i^-$ .

For spacelike geodesics, since  $a'(\eta) \neq 0$ , there is no ISG. For  $w < -1$ , NISGs do not reach  $\eta = 0$  or OE. For  $\eta = -\infty$ ,  $\lambda$  is determined by the integrals given by Eq. (A2). Thus, it is

finite for  $-5/3 < w < -1$  but goes to infinity for  $w \leq -5/3$ . From Eqs. (3.15) and (A2),  $\eta+r$  remains finite for  $-5/3 < w < -1$  but goes to infinity for  $w \leq -5/3$ . For  $-5/3 < w < -1$ ,  $A$  and  $B$  are bounded but  $(A+B)/a^2$  is unbounded. Therefore, for  $-5/3 < w < -1$ , the NISGs emanate from or terminate at a non-s.p. curvature singularity on ES but neither E nor S, while for  $w \leq -5/3$  they emanate from or terminate at E, spacelike infinity  $i^0$ . The coordinate  $\eta$  cannot approach any nonzero finite value as  $r \rightarrow \infty$ .

Finally, we consider ISCs. They are not geodesics in the flat case except for Minkowski spacetime. They have infinite g.a.p. in the limit E, which corresponds to spacelike infinity  $i^0$ .

The results for all cases with  $K = 0$  are summarised in Tables I and II. The Penrose diagrams are shown in Figs. 2 and 3, where the black solid, black dotted, black dashed-double-dotted, blue dashed-dotted and red dashed lines denote regular centres, extendible conformal boundaries, line-like conformal infinities, non-s.p. curvature singularities and s.p. curvature singularities, respectively, and black filled, black open and red open circles denote point-like extendible boundaries, infinities and s.p. curvature singularities, respectively. Figure 3 corrects the misidentification of ES with an extended boundary in Case F4a in Fig. 4 of Paper I.

Care is needed for future null infinity if  $a \rightarrow \infty$  and  $-1 < w < -1/3$ . In this case, since  $\rho \propto a^{-3(1+w)} \rightarrow 0$  but  $\rho a^2 \propto a^{-(1+3w)} \rightarrow \infty$ , a component of the Riemann tensor in the p.p. frame is unbounded in the infinite affine parameter limit. Since the curvature scale exceeds the Planck scale at some finite value of  $\lambda$ , quantum gravity effects may become significant and so the classical picture of spacetime breaks down. This feature is common to future null infinity with  $a \rightarrow \infty$  for  $-1 < w < -1/3$ ,  $K = 0, \pm 1$  and  $\rho > 0$ .

Care is also needed for spacelike infinity. Although a standard Penrose diagram applies for  $w > -1/3$ , no spacelike geodesic emanates from or terminates at the spacelike infinity E. This is because the integral on the right-hand side of Eq. (3.14) is finite if  $|\eta| < \infty$ . This is also the case for  $-5/3 < w \leq -1/3$  because the integral on the right-hand side of Eq. (3.15) is finite in the limit  $\eta \rightarrow -\infty$ . The above property of spacelike infinity also applies for that with  $K = -1$  for  $w > -5/3$  and  $\rho > 0$ .

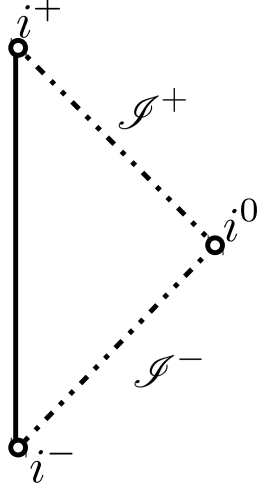


FIG. 2. The Penrose diagram for Minkowski spacetime, included for completeness.

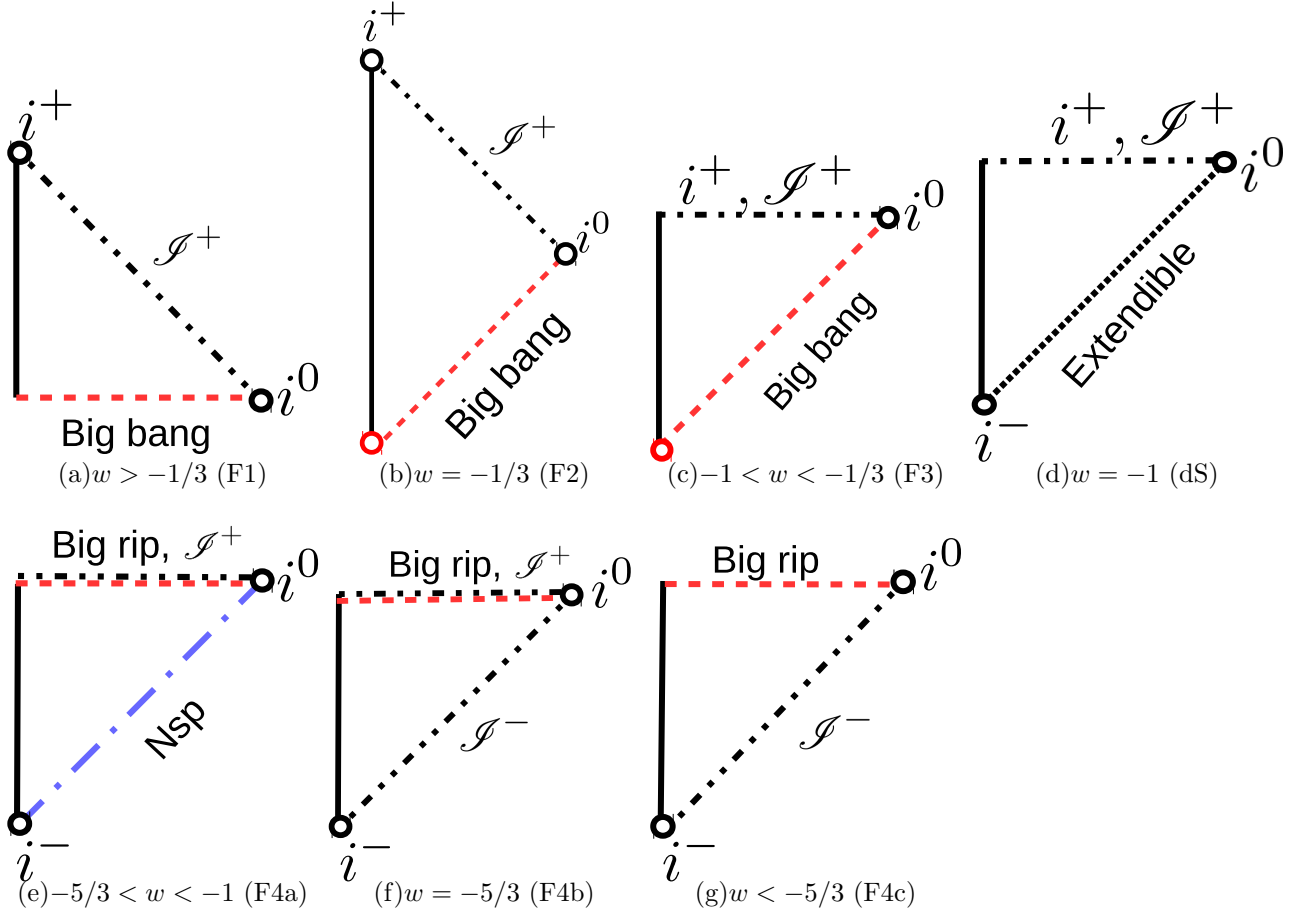


FIG. 3. The Penrose diagrams for flat FLRW solutions with the positive density.

TABLE I. Classification of geodesics in Minkowski spacetime. NG = null geodesic, CTG = comoving timelike geodesic, NCTG = non-comoving timelike geodesic, SG = spacelike geodesic.

Case	–	NG	CTG	NCTG	SG
Minkowski	Vacuum	ES( $\mathcal{I}^-$ ) $\rightarrow$ NE( $\mathcal{I}^+$ )	S( $i^-$ ) $\rightarrow$ N( $i^+$ )	S( $i^-$ ) $\rightarrow$ N( $i^+$ )	E( $i^0$ ) $\rightarrow$ E( $i^0$ )

TABLE II. Classification of geodesics in flat FLRW solutions. ext = extendible boundary, sp = s.p. curvature singularity, nsp = non-s.p. curvature singularity, dS = de Sitter spacetime.

Case	$w$	NG	CTG	NCTG	SG
F1	$(-1/3, \infty)$	OE(sp) $\rightarrow$ NE( $\mathcal{I}^+$ )	OE(sp) $\rightarrow$ N( $i^+$ )	OE(sp) $\rightarrow$ N( $i^+$ )	OE(sp) $\rightarrow$ OE(sp)
F2	$-1/3$	ES(sp) $\rightarrow$ NE( $\mathcal{I}^+$ )	S(sp) $\rightarrow$ N( $i^+$ )	ES(sp) $\rightarrow$ N( $i^+$ )	ES(sp) $\rightarrow$ ES(sp)
F3	$(-1, -1/3)$	ES(sp) $\rightarrow$ OE( $\mathcal{I}^+$ )	S(sp) $\rightarrow$ OE( $i^+$ )	ES(sp) $\rightarrow$ OE( $i^+$ )	ES(sp) $\rightarrow$ ES(sp)
dS	$-1$	ES(ext) $\rightarrow$ OE( $\mathcal{I}^+$ )	S( $i^-$ ) $\rightarrow$ OE( $i^+$ )	ES(ext) $\rightarrow$ OE( $i^+$ )	ES(ext) $\rightarrow$ ES(ext)
F4a	$(-5/3, -1)$	ES(nsp) $\rightarrow$ OE( $\mathcal{I}^+$ )	S( $i^-$ ) $\rightarrow$ OE(sp)	ES(nsp) $\rightarrow$ OE(sp)	ES(nsp) $\rightarrow$ ES(nsp)
F4b	$-5/3$	ES( $\mathcal{I}^-$ ) $\rightarrow$ OE( $\mathcal{I}^+$ )	S( $i^-$ ) $\rightarrow$ OE(sp)	S( $i^-$ ) $\rightarrow$ OE(sp)	E( $i^0$ ) $\rightarrow$ E( $i^0$ )
F4c	$(-\infty, -5/3)$	ES( $\mathcal{I}^-$ ) $\rightarrow$ OE(sp)	S( $i^-$ ) $\rightarrow$ OE(sp)	S( $i^-$ ) $\rightarrow$ OE(sp)	E( $i^0$ ) $\rightarrow$ E( $i^0$ )

### C. Positive-Curvature FLRW solutions

For  $K = 1$ , if  $w \neq -1/3$ , the solution is time-symmetric. The asymptotic behaviour of  $a(\eta)$  at  $\eta = 0$  and  $\eta = \eta_c = 2\pi/(1 + 3w)$  coincides with that of flat FLRW at  $\eta = 0$ . The analysis of causal geodesics is straightforward. The behaviour of spacelike geodesics is rather complicated. There exists an ISG at  $\eta = \eta_m = \pi/(1 + 3w)$ , which goes around the 3-sphere infinitely many times in an infinitely large affine parameter. For  $w > -1/3$ , NISGs with  $|C| > a(\eta_m)$  emanate from the big-bang singularity at  $\eta = 0$  and terminate at the big-crunch singularity at  $\eta = \eta_c$ , NISGs with  $|C| < a(\eta_m)$  emanate from the big-bang singularity, bounce back and return to the big-bang singularity or behave like their time reversal with respect to  $\eta = \eta_m$ , and NISGs with  $|C| = a(\eta_m)$  emanate from the big-bang and approach  $\eta = \eta_m$ , turning around the 3-sphere infinitely many times in an infinitely large affine parameter, or behave as their time reversal with respect to  $\eta = \eta_m$ . For  $w < -1/3$ , NISGs oscillate with respect to  $\eta$  infinitely many times between  $\eta_+$  and  $\eta_- = \eta_c - \eta_+$ , where  $a(\eta_{\pm}) = |C|$ , and turn around the 3-sphere infinitely many times in an infinitely large affine

parameter.

The  $w = -1/3$  case requires special treatment. For  $a = b_c e^{b_c \eta}$  (Case P2a), the analysis is essentially the same as for the flat solution with  $w = -1/3$  except for the spatial spherical topology. There is no ISG, while NISGs emanate from and terminate at the big-bang singularity. For  $a = a_0 = \text{const}$  (Case P2b), the spacetime is given by the exact Einstein static model. In this case, all geodesics are complete. There are ISGs at any constant  $\eta$  and NISGs, both of which turn around the 3-sphere infinitely many times in an infinitely large affine parameter. The results for all cases are summarised in Table III, where spacelike geodesics are omitted because of their complicated behaviour. The resultant Penrose diagrams are shown in Fig. 4. Figure 4 improves Fig. 5 of Paper I by clarifying both  $i^\pm$  and  $\mathcal{I}^\pm$ .

TABLE III. Classification of causal geodesics in positive-curvature FLRW solutions. Cases P2a and P2b are an expanding solution and a static solution, respectively. See text for spacelike geodesics.

Case	$w$	NG	CTG	NCTG
P1	$(-1/3, \infty)$	OE(sp) $\rightarrow$ NA(sp)	OE(sp) $\rightarrow$ NA(sp)	OE(sp) $\rightarrow$ NA(sp)
P2a	$-1/3$	S(sp) $\rightarrow$ N( $\mathcal{I}^+$ )	S(sp) $\rightarrow$ N( $i^+$ )	S(sp) $\rightarrow$ N( $i^+$ )
P2b	$-1/3$	S( $\mathcal{I}^-$ ) $\rightarrow$ N( $\mathcal{I}^+$ )	S( $i^-$ ) $\rightarrow$ N( $i^+$ )	S( $i^-$ ) $\rightarrow$ N( $i^+$ )
P3	$(-1, -1/3)$	SB( $\mathcal{I}^-$ ) $\rightarrow$ OE( $\mathcal{I}^+$ )	SB( $i^-$ ) $\rightarrow$ OE( $i^+$ )	SB( $i^-$ ) $\rightarrow$ OE( $i^+$ )
dS	$-1$	SB( $\mathcal{I}^-$ ) $\rightarrow$ OE( $\mathcal{I}^+$ )	SB( $i^-$ ) $\rightarrow$ OE( $i^+$ )	SB( $i^-$ ) $\rightarrow$ OE( $i^+$ )
P4a	$[-5/3, -1)$	SB( $\mathcal{I}^-$ ) $\rightarrow$ OE( $\mathcal{I}^+$ )	SB(sp) $\rightarrow$ OE(sp)	SB(sp) $\rightarrow$ OE(sp)
P4b	$(-\infty, -5/3)$	SB(sp) $\rightarrow$ OE(sp)	SB(sp) $\rightarrow$ OE(sp)	SB(sp) $\rightarrow$ OE(sp)

#### D. Negative-Curvature FLRW solutions with $\rho \geq 0$

The vacuum solution is Milne spacetime and there is no curvature singularity. Since  $a = e^\eta$ , the behaviour of geodesics is the same as for the flat case with  $w = -1/3$ . This behaviour is summarised in Table IV and the Penrose diagram is shown in Fig. 5.

For  $\rho > 0$ , we first consider  $w \neq -1/3$ . Since  $a \propto \eta^\alpha$  in the limit  $\eta \rightarrow 0$ , the behaviour of geodesics is the same as in the flat case with the same  $w$  in this limit. The p.p.-frame components of the Riemann tensor have the same behaviour as in the flat case. In the limit

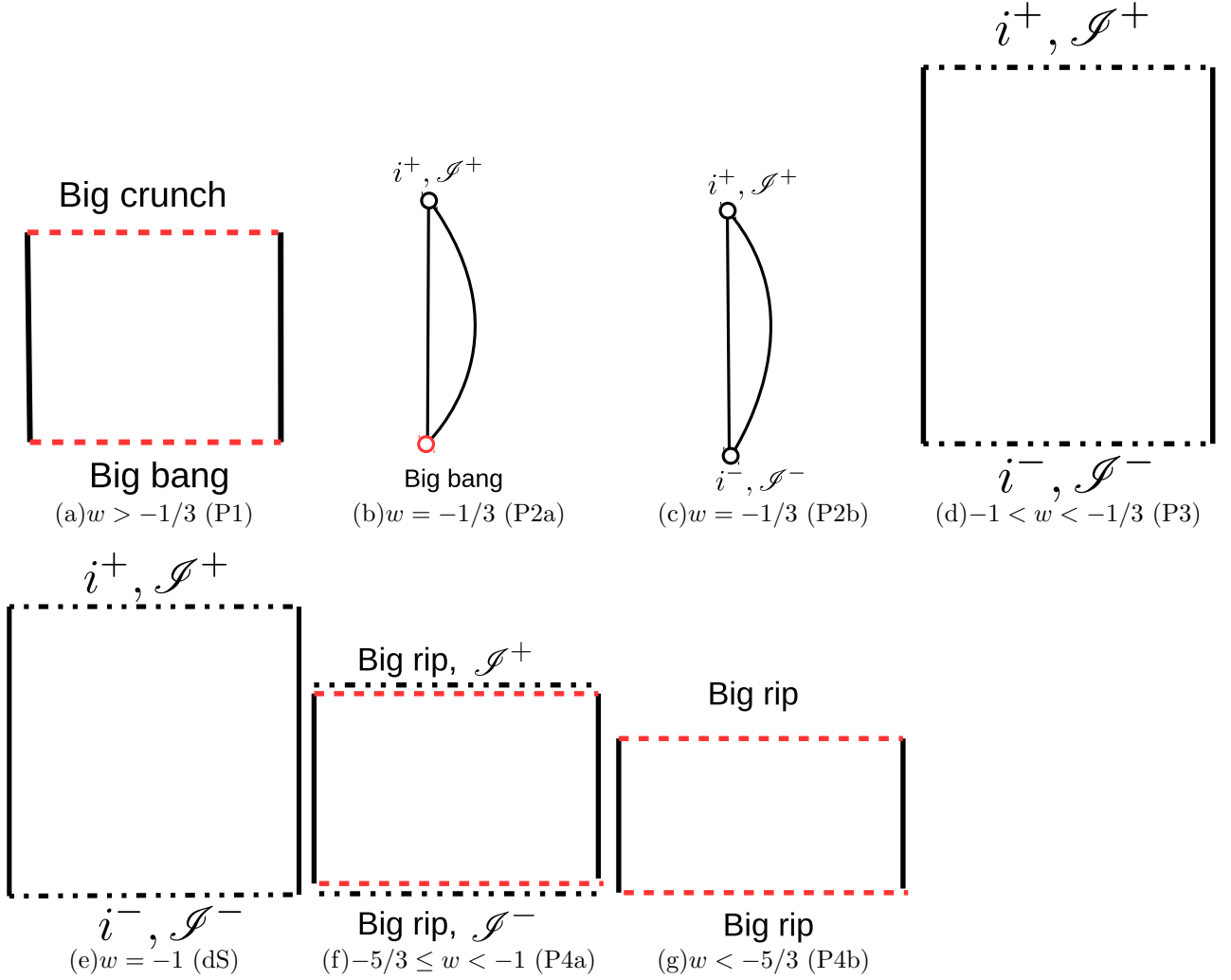


FIG. 4. The Penrose diagrams for positive-curvature FLRW solutions.

TABLE IV. Classification of geodesics in Milne spacetime.

Case	–	NG	CTG	NCTG	SG
Milne	Vacuum	ES(ext) $\rightarrow$ NE( $\mathcal{I}^+$ )	S(ext) $\rightarrow$ N( $i^+$ )	ES(ext) $\rightarrow$ N( $i^+$ )	ES(ext) $\rightarrow$ ES(ext)

$\tilde{\eta} \rightarrow \infty$ , since

$$\tilde{a} \approx \tilde{a}_c \frac{e^{\tilde{\eta}}}{4}, \quad \eta = \frac{1}{1+3w} \tilde{\eta} \quad (4.3)$$

and  $\tilde{a} = a^{1+3w}$ , we find

$$a \propto e^{\eta}. \quad (4.4)$$

This behaviour is the same as in the flat case with  $w = -1/3$ . Therefore, if  $w > -1/3$ , in the limit  $\eta \rightarrow \infty$ ,  $a \rightarrow \infty$  and all causal geodesics are future complete. All NCTGs terminate at

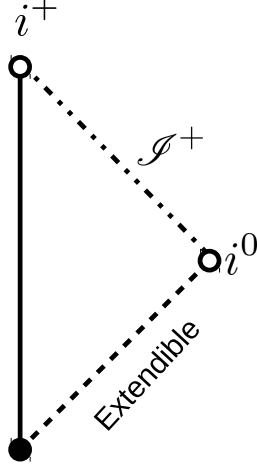


FIG. 5. The Penrose diagram for Milne spacetime.

N. For  $w < -1/3$ , in the limit  $\eta \rightarrow -\infty$ ,  $a \rightarrow 0$  and all causal geodesics are past incomplete. NCTGs emanate from ES but neither E nor S. For  $w = -1/3$ , the behaviour of geodesics is the same as in the flat case with  $w = -1/3$ .

The results for all negative-curvature FLRW solutions for  $\rho \geq 0$  are summarised in Table V and the Penrose diagrams are shown in Fig. 6. This corrects the misidentification of ES with an extendible boundary in Case NP4a in Fig. 7 of Paper I.

TABLE V. Classification of geodesics in negative-curvature FLRW solutions with  $\rho > 0$ .

Case	$w$	NG	CTG	NCTG	SG
NP1	$(-1/3, \infty)$	OE(sp) $\rightarrow$ NE( $\mathcal{I}^+$ )	OE(sp) $\rightarrow$ N( $i^+$ )	OE(sp) $\rightarrow$ N( $i^+$ )	OE(sp) $\rightarrow$ OE(sp)
NP2	$-1/3$	ES(sp) $\rightarrow$ NE( $\mathcal{I}^+$ )	S(sp) $\rightarrow$ N( $i^+$ )	ES(sp) $\rightarrow$ N( $i^+$ )	ES(sp) $\rightarrow$ ES (sp)
NP3	$(-1, -1/3)$	ES(sp) $\rightarrow$ OE( $\mathcal{I}^+$ )	S(sp) $\rightarrow$ OE( $i^+$ )	ES(sp) $\rightarrow$ OE( $i^+$ )	ES(sp) $\rightarrow$ ES(sp)
dS	$-1$	ES(ext) $\rightarrow$ OE( $\mathcal{I}^+$ )	S(ext) $\rightarrow$ OE( $i^+$ )	ES(ext) $\rightarrow$ OE( $i^+$ )	ES(ext) $\rightarrow$ ES(ext)
NP4a	$(-5/3, -1)$	ES(nsp) $\rightarrow$ OE( $\mathcal{I}^+$ )	S(ext) $\rightarrow$ OE(sp)	ES(nsp) $\rightarrow$ OE(sp)	ES(nsp) $\rightarrow$ ES(nsp)
NP4b	$-5/3$	ES(ext) $\rightarrow$ OE( $\mathcal{I}^+$ )	S(ext) $\rightarrow$ OE(sp)	ES(ext) $\rightarrow$ OE(sp)	ES(ext) $\rightarrow$ ES(ext)
NP4c	$(-\infty, -5/3)$	ES(ext) $\rightarrow$ OE(sp)	S(ext) $\rightarrow$ OE(sp)	ES(ext) $\rightarrow$ OE(sp)	E( $i^0$ ) $\rightarrow$ E( $i^0$ )

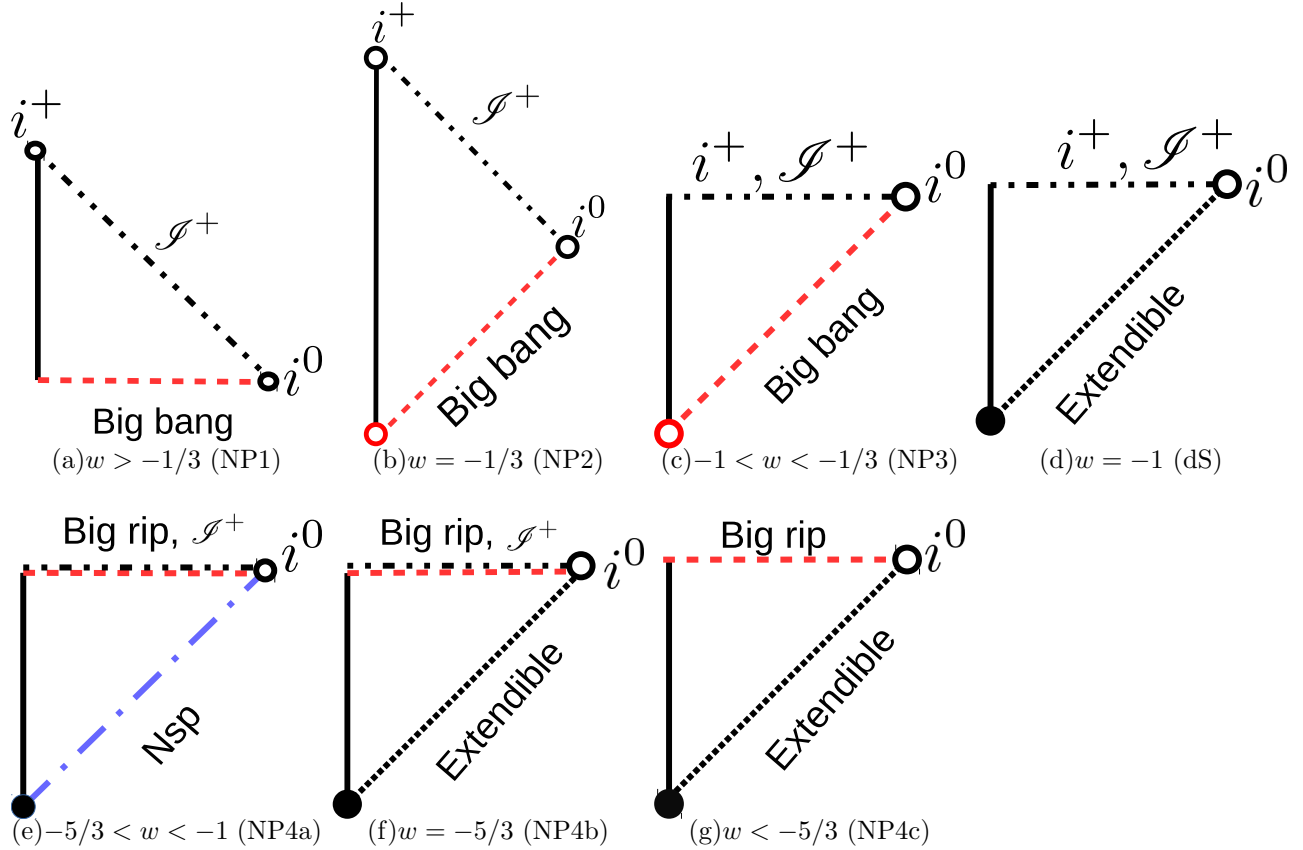


FIG. 6. The Penrose diagrams for negative-curvature FLRW solutions with the positive density.

### E. Negative-Curvature FLRW solutions with $\rho < 0$

We first consider  $w \neq -1/3$ . In this case, the solution is time-symmetric. In the limit  $\tilde{\eta} \rightarrow \pm\infty$ , since  $\tilde{a} \propto e^{|\tilde{\eta}|}$ , we have  $a \propto e^{\text{sgn}(1+3w)|\eta|}$ . For  $w > -1/3$  and  $\eta \rightarrow \pm\infty$ , all causal geodesics are complete. Both CTGs and NCTGs emanate from S, a past timelike infinity, and terminate at N, a future timelike infinity. The null boundaries NE and ES are future and past null infinities, respectively. For  $w < -1/3$  and  $\eta \rightarrow \pm\infty$ , all causal geodesics are incomplete. Since  $\rho \propto a^{-3(1+w)}$ , CTGs emanate from S, a big-bang singularity, and terminate at N, a big-crunch singularity, for  $-1 < w < -1/3$  but the spacetime is extendible beyond S and N for  $w \leq -1$ . Both null geodesics and NCTGs emanate from ES but neither E nor S and terminate at NE but neither N nor E. Since  $\rho \propto a^{-3(1+w)}$ ,  $\rho a^2 \propto a^{-(1+3w)}$  and  $\rho/a^2 \propto a^{-(5+3w)}$ , the null boundaries NE and ES are, respectively, big-bang and big-crunch singularities for  $-1 < w < -1/3$ , non-s.p. curvature null singularities for  $-5/3 < w < -1$ , and extendible boundaries for  $w = -1$  and  $w \leq -5/3$ . The behaviour of spacelike geodesics

is rather complicated. There exists an ISG at  $\eta = 0$ , which emanates from and terminates at spacelike infinity E. The behaviour of NISGs for  $w > -1/3$  ( $w < -1/3$ ) corresponds to that in the positive-curvature case for  $w < -1/3$  ( $w > -1/3$ ). The difference is in open hyperbolic spatial geometry with future and past null boundaries in place of a 3-sphere with future and past spacelike boundaries.

Next we consider  $w = -1/3$ . For  $0 < \tilde{a}'_c < 1$  (Case NN2a), the behaviour of the scale factor  $a$  and the geodesics is the same as in the flat case with  $w = -1/3$ . There is no ISG, while NISGs emanate from and terminate at a big-bang null singularity ES. For  $\tilde{a}'_c = 1$  (Case NN2b), the spacetime is static and there is no curvature singularity. All geodesics are complete. There are ISGs at any constant  $\eta$  and all NISGs emanate from and terminate at spacelike infinity E.

The results for all negative-curvature FLRW solutions with  $\rho < 0$  are summarised in Table VI, where spacelike geodesics are omitted and the Penrose diagrams are shown in Fig. 7. This corrects the misidentification of NE and ES with extendible boundaries in Fig. 8 of Paper I.

TABLE VI. Classification of causal geodesics in negative-curvature FLRW solutions with  $\rho < 0$ . Cases NN2a and NN2b are an expanding and static solutions, respectively. See text for spacelike geodesics. AdS = anti-de Sitter spacetime.

Case	$w$	NG	CTG	NCTG
NN1	$(-1/3, \infty)$	$\text{ES}(\mathcal{I}^-) \rightarrow \text{NE}(\mathcal{I}^+)$	$\text{S}(i^-) \rightarrow \text{N}(i^+)$	$\text{S}(i^-) \rightarrow \text{N}(i^+)$
NN2a	$-1/3$	$\text{ES}(\text{sp}) \rightarrow \text{NE}(\mathcal{I}^+)$	$\text{S}(\text{sp}) \rightarrow \text{N}(i^+)$	$\text{ES}(\text{sp}) \rightarrow \text{N}(i^+)$
NN2b	$-1/3$	$\text{ES}(\mathcal{I}^-) \rightarrow \text{NE}(\mathcal{I}^+)$	$\text{S}(i^-) \rightarrow \text{N}(i^+)$	$\text{S}(i^-) \rightarrow \text{N}(i^+)$
NN3	$(-1, -1/3)$	$\text{ES}(\text{sp}) \rightarrow \text{NE}(\text{sp})$	$\text{S}(\text{sp}) \rightarrow \text{N}(\text{sp})$	$\text{ES}(\text{sp}) \rightarrow \text{NE}(\text{sp})$
AdS	$-1$	$\text{ES}(\text{ext}) \rightarrow \text{NE}(\text{ext})$	$\text{S}(\text{ext}) \rightarrow \text{N}(\text{ext})$	$\text{ES}(\text{ext}) \rightarrow \text{NE}(\text{ext})$
NN4a	$(-5/3, -1)$	$\text{ES}(\text{nsp}) \rightarrow \text{NE}(\text{nsp})$	$\text{S}(\text{ext}) \rightarrow \text{N}(\text{ext})$	$\text{ES}(\text{nsp}) \rightarrow \text{NE}(\text{nsp})$
NN4b	$(-\infty, -5/3]$	$\text{ES}(\text{ext}) \rightarrow \text{NE}(\text{ext})$	$\text{S}(\text{ext}) \rightarrow \text{N}(\text{ext})$	$\text{ES}(\text{ext}) \rightarrow \text{NE}(\text{ext})$

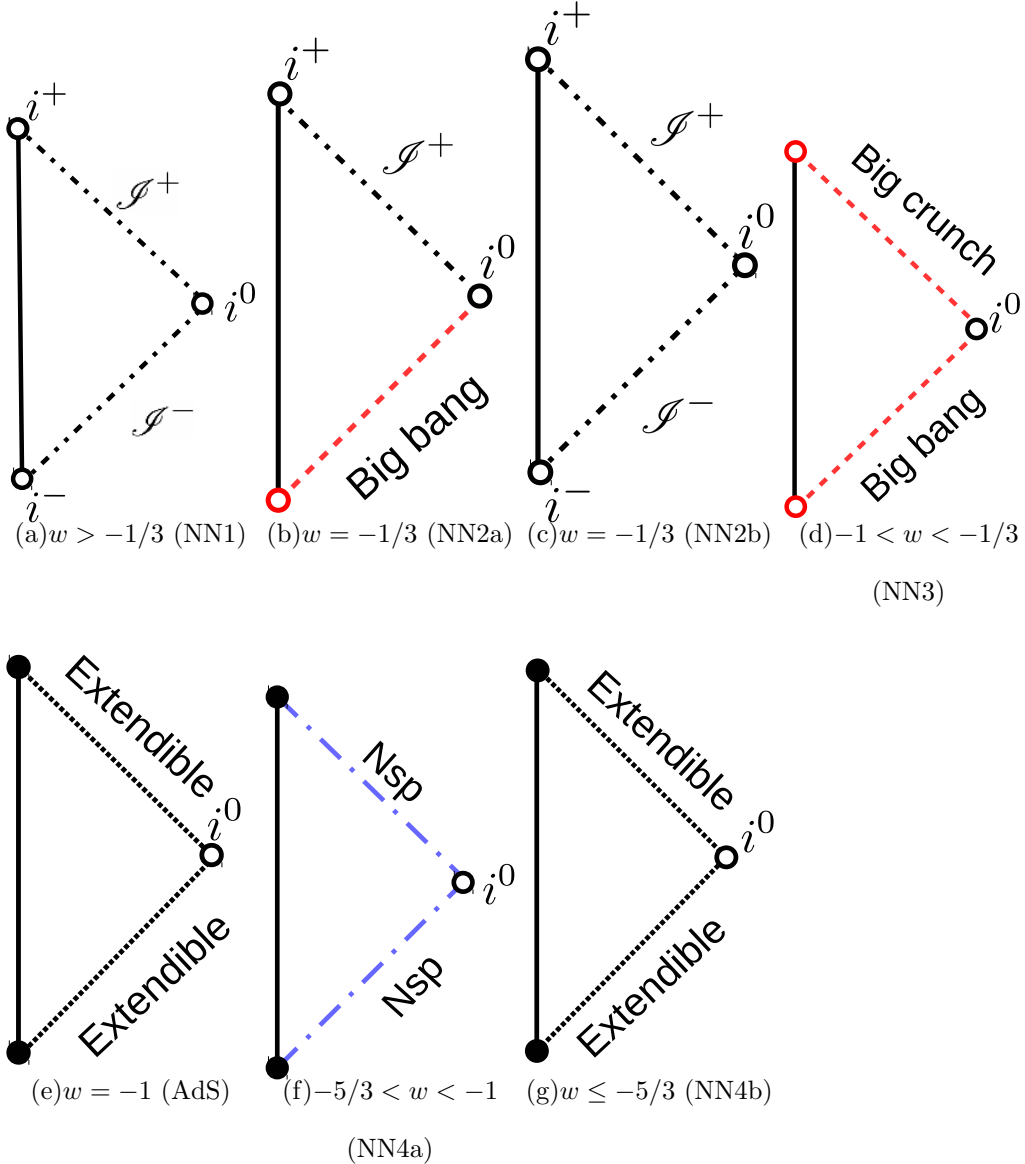


FIG. 7. The Penrose diagrams for negative-curvature FLRW solutions with the negative density.

## V. SUMMARY

Extending the analysis in Paper I [20] to include general geodesics, instantaneous space-like curves and p.p. curvature singularities, we have classified all geodesics and conformal boundaries in the FLRW solutions with the linear equation of state  $p = w\rho$  but without assuming any energy conditions. We have found that there is unexpected rich structure of conformal boundaries for  $w \leq -1/3$ , while the standard well-known structure of conformal boundaries is recovered for  $w > -1/3$ . For  $w > -5/3$  and  $\rho > 0$ , no spacelike geodesic

emanates from or terminates at the spacelike infinity in the flat and negative-curvature cases. For  $\rho > 0$  and  $w < -1$ , the spacetime commonly ends with a future big-rip spacelike singularity, although for  $-5/3 \leq w < -1$ , it is still future null geodesically complete. In the flat and negative-curvature cases with  $\rho > 0$ , the expanding universe begins with a big-bang spacelike singularity for  $w > -1/3$ , a big-bang null singularity for  $-1 < w \leq -1/3$  and a non-s.p. curvature null singularity for  $-5/3 < w < -1$ . This implies that no quasi-exponential inflationary model avoids the initial singularity problem if it is described by the flat or negative-curvature solutions with  $-5/3 < w < -1$  or  $-1 < w < -1/3$ . For  $w \leq -5/3$ , the flat and negative-curvature solutions have a past null infinity and a past extendible null boundary, respectively. For  $K = 1$  and  $w < -1/3$ , the solution describes a bouncing universe, which is singularity-free for  $-1 \leq w < -1/3$  but has past and future big-rip singularities for  $w < -1$ . Although nature of the matter that corresponds to  $w = -5/3$  is not clear, the Einstein equation suggests that this value is just as critical as  $1/3$ ,  $-1/3$  and  $-1$ .

## ACKNOWLEDGMENTS

The authors are very grateful to T. Hiramatsu, A. Ishibashi, M. Kimura, H. Maeda, J. M. M. Senovilla, C.-M. Yoo and D. Yoshida for fruitful discussion. This work was partially supported by JSPS KAKENHI Grant Numbers JP19K03876, JP19H01895, JP20H05853 (TH) and JP19K14715 (TI).

## Appendix A: Integrals

The following are integrals used in the analysis of geodesics for flat FLRW solutions.

$$\int_{\eta_0}^{\eta} a(\tilde{\eta}) d\tilde{\eta} = \begin{cases} \frac{1}{1+\alpha} b_0 (\eta^{1+\alpha} - \eta_0^{1+\alpha}) & (w > -1/3) \\ e^{b_c \eta} - e^{b_c \eta_0} & (w = -1/3) \\ -\frac{1}{1+\alpha} b_0 [(-\eta)^{1+\alpha} - (-\eta_0)^{1+\alpha}] & (w < -1, -1 < w < -1/3) \\ -b_0 [\ln(-\eta) - \ln(-\eta_0)] & (w = -1) \end{cases}, \quad (\text{A1})$$

$$\int_{\eta_0}^{\eta} a^2(\tilde{\eta}) d\tilde{\eta} = \begin{cases} \frac{1}{1+2\alpha} b_0^2 (\eta^{1+2\alpha} - \eta_0^{1+2\alpha}) & (w > -1/3) \\ \frac{b_c}{2} (e^{2b_c \eta} - e^{2b_c \eta_0}) & (w = -1/3) \\ -\frac{1}{1+2\alpha} b_0^2 [(-\eta)^{1+2\alpha} - (-\eta_0)^{1+2\alpha}] & (w < -5/3, -5/3 < w < -1/3) \\ -b_0^2 [\ln(-\eta) - \ln(-\eta_0)] & (w = -5/3) \end{cases}. \quad (\text{A2})$$

- 
- [1] R. M. Wald, *General Relativity* (The University of Chicago Press, Chicago, 1984).
  - [2] T. M. C. Abbott *et al.* (DES Collaboration), *Phys. Rev. D* **98** (2018) 043526 [arXiv:1708.01530 [astro-ph.CO]].
  - [3] P. A. R. Ade *et al.* (Planck Collaboration), *Astron. Astrophys.* **594** (2016) A13 [arXiv:1502.01589 [astro-ph.CO]].
  - [4] R. R. Caldwell, R. Dave and P. J. Steinhardt, *Phys. Rev. Lett.* **80** (1998) 1582 [arXiv:astro-ph/9708069].
  - [5] I. Zlatev, L. Wang and P. J. Steinhardt, *Phys. Rev. Lett.* **82** (1999) 896 [arXiv:astro-ph/9807002].
  - [6] R. R. Caldwell, *Phys. Lett. B* **545** (2002) 23 [arXiv:astro-ph/9908168].
  - [7] T. Kobayashi, *Rep. Prog. Phys.* **82** (2019) 086901 [arXiv:1901.07183 [gr-qc]].
  - [8] J. R. Oppenheimer and H. Snyder, *Phys. Rev.* **56** (1939) 455.
  - [9] B. J. Carr, *Astrophys. J.* **201** (1975) 1.
  - [10] T. Harada, C. M. Yoo and K. Kohri, *Phys. Rev. D* **88** (2013) 084051 [erratum: *Phys. Rev. D* **89** (2014) 029903] [arXiv:1309.4201 [astro-ph.CO]].
  - [11] P. O. Mazur and E. Mottola, *Proc. Nat. Acad. Sci. U.S.A.* **101** (2004) 9545 [arXiv:gr-qc/0407075].

- [12] M. Visser and D. L. Wiltshire, *Classical Quantum Gravity* **21** (2004) 1135 [arXiv:gr-qc/0310107].
- [13] J. M. M. Senovilla, *Gen. Relativ. Gravit.* **30** (1998) 701 [arXiv:1801.04912 [gr-qc]].
- [14] R. R. Caldwell, M. Kamionkowski and N. N. Weinberg, *Phys. Rev. Lett.* **91** (2003) 071301 [arXiv:astro-ph/0302506].
- [15] M. P. Dabrowski, T. Stachowiak and M. Szydlowski, *Phys. Rev. D* **68**, 103519 (2003) [arXiv:hep-th/0307128 [hep-th]].
- [16] M. P. Dabrowski and T. Stachowiak, *Annals Phys.* **321**, 771-812 (2006) [arXiv:hep-th/0411199 [hep-th]].
- [17] L. Fernandez-Jambrina and R. Lazkoz, *Phys. Rev. D* **74** (2006) 064030 [arXiv:gr-qc/0607073].
- [18] D. Yoshida and J. Quintin, *Classical Quantum Gravity* **35** (2018) 155019 [arXiv:1803.07085 [gr-qc]].
- [19] K. Nomura and D. Yoshida, *J. Cosmol. Astropart. Phys.* 07 (2021) 047 [arXiv:2105.05642 [gr-qc]].
- [20] T. Harada, B. J. Carr and T. Igata, *Classical Quantum Gravity* **35** (2018) 105011 [arXiv:1801.01966 [gr-qc]].
- [21] S. W. Hawking and G. F. R. Ellis, *The Large Scale Structure of Space-Time* (Cambridge University Press, Cambridge, England, 1973).
- [22] C. J. S. Clarke, *The Analysis of space-time singularities*, Cambridge Lecture Notes in Physics **1** (Cambridge University Press, Cambridge, England, 1994).